

## Quantification of excess vacancy defects from high-energy ion implantation in Si by Au labeling

R. Kalyanaraman<sup>a)</sup> and T. E. Haynes

*Solid State Division, Oak Ridge National Laboratory, Oak Ridge, Tennessee 37831*

V. C. Venezia, D. C. Jacobson, H.-J. Gossmann, and C. S. Rafferty

*Bell Laboratories, Lucent Technologies, Murray Hill, New Jersey 07974*

(Received 13 March 2000; accepted for publication 12 April 2000)

It has been shown recently that Au labeling [V. C. Venezia, D. J. Eaglesham, T. E. Haynes, A. Agarwal, D. C. Jacobson, H.-J. Gossmann, and F. H. Baumann, *Appl. Phys. Lett.* **73**, 2980 (1998)] can be used to profile vacancy-type defects located near half the projected range ( $\frac{1}{2}R_p$ ) in MeV-implanted Si. In this letter, we have determined the ratio of vacancies annihilated to Au atoms trapped (calibration factor “ $k$ ”) for the Au-labeling technique. The calibration experiment consisted of three steps: (1) a 2 MeV  $\text{Si}^+$  implant into Si(100) followed by annealing at 815 °C to form stable excess vacancy defects; (2) controlled injection of interstitials in the  $\frac{1}{2}R_p$  region of the above implant via 600 keV  $\text{Si}^+$  ions followed by annealing to dissolve the {311} defects; and (3) Au labeling. The reduction in Au concentration in the near-surface region (0.1–1.6  $\mu\text{m}$ ) with increasing interstitial injection provides the most direct evidence so far that Au labeling detects the vacancy-type defects. By correlating this reduction in Au with the known number of interstitials injected, it was determined that  $k = 1.2 \pm 0.2$  vacancies per trapped Au atom. © 2000 American Institute of Physics. [S0003-6951(00)00723-3]

Renewed interest in the use of high-energy ion implantation (HEI) in Si as a cost-effective device processing step<sup>1,2</sup> has created a serious need to understand defects resulting from such implants. In particular, the higher average forward momentum of recoiled atoms produced in the collision cascades results in an excess of vacancy-type defects in the shallow part of the implant profile.<sup>3</sup> While interstitial-type defects at the projected range ( $R_p$ ) of the implants in Si have been well studied,<sup>4</sup> much less is known about defects in the near-surface region of these implants. The reason for this is primarily due to the inability of current techniques to reliably detect or quantify vacancy-type defects. In this work, we show that it is possible to not only detect but also quantify vacancy-type defects in Si using the Au-labeling technique previously described by Venezia and co-workers.<sup>5</sup> Controlled vacancy removal and counting was achieved in a three-step experiment. First, stable vacancy-type defects were formed by a 2 MeV  $\text{Si}^+$  implant and anneal.<sup>5</sup> Second, controlled vacancy removal was achieved by medium-energy (600 keV)  $\text{Si}^+$  implants of various doses followed by a second anneal (+I *implant and anneal*). The third and final step was to measure the change in vacancy concentration by saturating the Au in the  $\frac{1}{2}R_p$  region by Au labeling. The vacancy removal results in less Au being trapped afterward. Correlation of the concentration of trapped Au with the number of vacancies removed provides a measurement of the calibration factor  $k$ , which is the ratio of vacancies annihilated to Au atoms trapped in the Au-labeled profiles. This determination of  $k$  allows unambiguous, quantitative measurement of the vacancy concentrations produced by high-energy implantation in Si.

In 1996, Holland and co-workers<sup>6</sup> showed from transmission electron microscopy (TEM) studies that extended vacancy-type defects form in the near-surface region for extremely high-dose implants. Other groups extended this finding of vacancy-type defects to more moderate implantation doses via x-ray diffraction strain measurements<sup>7</sup> and positron annihilation spectroscopy (PAS)  $S$ -parameter measurements.<sup>8</sup> These findings suggest that precursors to the large open-volume defects of the Holland *et al.* work<sup>6</sup> are the free vacancies resulting from the displacement of interstitials with respect to vacancies occurring in heavy-ion and/or high-energy implants. Presently, techniques like PAS, x-ray strain measurements, and TEM are capable of detecting vacancy-type defects, but cannot accurately quantify the concentration of vacancies present. While TEM is capable of quantitative measurements of open-volume defects of large sizes, small vacancy clusters are difficult to detect. More recently, cross-section x-ray diffuse scattering<sup>9</sup> has been used to make a quantitative estimate of excess vacancy-type defects from a 10 MeV Si self-implant. While it is, in principle, possible to deconvolute the defect size and concentration by diffuse scattering, this has not yet been accomplished for HEI in the energy range of interest. Recently, Venezia *et al.*<sup>5</sup> used gettering of Au atoms to obtain depth profiles of the defects in the  $\frac{1}{2}R_p$  region of MeV self-implants in Si. The motivation for using Au was based on two principal factors: (a) the kick-out mechanism<sup>10</sup> that controls diffusion of Au in Si implies that Au will be trapped in the vicinity of interstitial sinks, including vacancy-type defects, and (b) the good sensitivity of Rutherford backscattering (RBS) to detect Au in Si. In this work, we establish the quantitative capability of this technique to profile the concentration of vacancies in the near-surface region formed by a 2 MeV self-implant in Si.

<sup>a)</sup>Electronic mail: ramkik@lucent.com

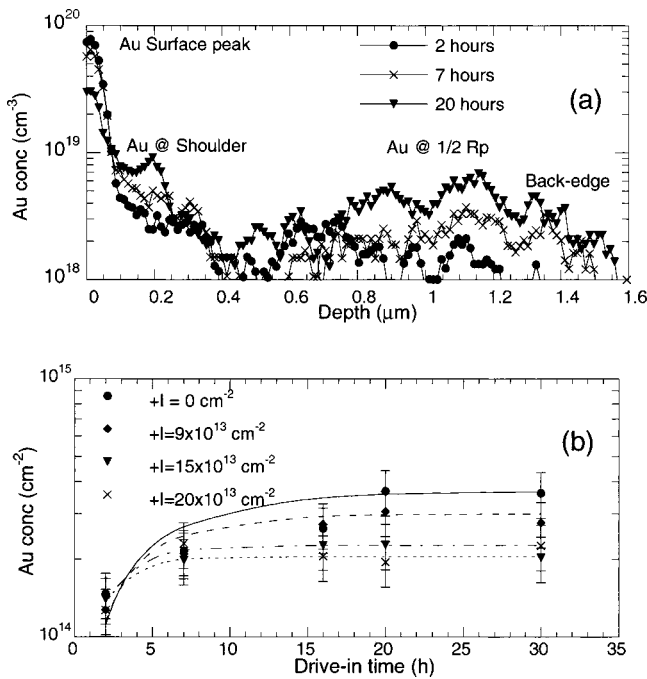


FIG. 1. (a) RBS profiles of Au concentration in the HEI sample for various Au drive-in times. (b) Au concentration at  $\frac{1}{2}R_p$  (0.5–1.6  $\mu\text{m}$ ) vs drive-in time. Smooth curves are fits of type  $C_0(1 - \exp^{-t/\tau})$ . Error bars are  $\pm 20\%$ .

*P*-type float-zone Si(100) ( $\rho = 65\text{--}80\ \Omega\ \text{cm}$ ) wafers were first implanted with 2 MeV Si ( $R_p \sim 2\ \mu\text{m}$ ) with a dose of  $1 \times 10^{16}\ \text{cm}^{-2}$  at an angle of  $7^\circ$  from the surface-normal direction using a 1.7 MeV National Electrostatics tandem Pelletron. The substrate temperature during the implant was maintained at  $70\text{--}80^\circ\text{C}$ , while the chamber pressure was between  $2$  and  $5 \times 10^{-6}$  Torr. The implanted samples were then furnace annealed at  $815^\circ\text{C}$  for 20 min (henceforth, referred to as the *HEI sample*) in 1 atm of argon. After this anneal, interstitial injection was carried out by implanting 600 keV Si<sup>+</sup> ions at doses from  $5 \times 10^{13}$  to  $20 \times 10^{13}\ \text{cm}^{-2}$  followed by a  $765^\circ\text{C}$ , 20 min anneal in flowing Ar. The projected range of this implant is  $\sim 0.9\ \mu\text{m}$  [from SRIM-2000 (Ref. 11)], which puts it almost at  $\frac{1}{2}R_p$  of the 2 MeV Si<sup>+</sup> implant. The dose range for the +I implant was chosen to stay below the threshold dose for forming dislocation loops in order to ensure that any clusters or extended defects containing interstitials would be completely dissolved in the  $765^\circ\text{C}$  anneal. Finally, the Au labeling was carried out by implanting Au at 68 keV ( $R_p \sim 0.03\ \mu\text{m}$ ) and  $8 \times 10^{14}\ \text{cm}^{-2}$  dose in the HEI samples and the HEI+I samples. The implanted Au was diffused in at  $750^\circ\text{C}$  in 1 atm of argon for times up to 30 h. The Au concentration profiles were then measured by RBS in random geometry, using 2.8 MeV  $^4\text{He}^{2+}$  at an incident angle of  $22^\circ$  relative to the surface-normal direction with the detector at  $170^\circ$  from the incident ion direction.

Figure 1(a) shows typical RBS profiles of Au in the near-surface region of the HEI samples for different Au indiffusion times. Besides the Au-implant peak at the surface, a broad peak appears in the  $\frac{1}{2}R_p$  region around  $\sim 0.5\text{--}1.6\ \mu\text{m}$  as well as a narrower ‘‘shoulder,’’<sup>12</sup> peak near  $0.2\ \mu\text{m}$ . As the data show, there is a substantial increase in Au at both the shoulder and  $\frac{1}{2}R_p$  in going from 2 to 20 h of Au drive-in time, indicating that the Au concentration takes considerable time to saturate for a HEI dose of  $1 \times 10^{16}\ \text{cm}^{-2}$ . With re-

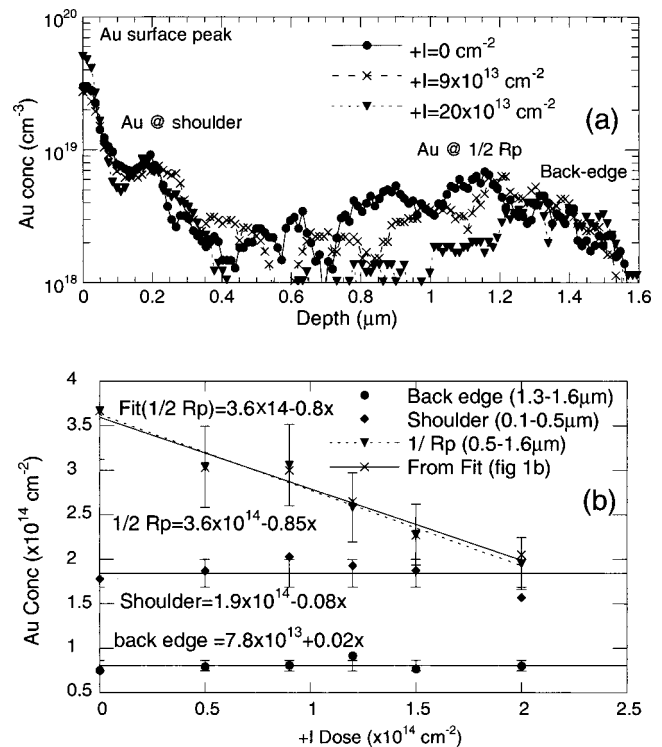


FIG. 2. (a) RBS profiles of Au concentration after 20 h drive-in for various +I doses. (b) Au concentration vs +I dose. Error bars on back-edge and shoulder data are  $\pm 1\sigma$  and those on  $\frac{1}{2}R_p$  are  $\pm 10\%$ .

spect to the earlier qualitative work by Venezia *et al.*,<sup>5</sup> accurate quantification of this technique required that the Au and vacancy-type defect interaction be taken to completion. The saturation characteristics of the Au profiles in the  $\frac{1}{2}R_p$  region (0.5–1.6  $\mu\text{m}$ ) for the HEI sample and with various +I doses are plotted as a function of time in Fig. 1(b). The smooth curves in Fig. 1(b) are exponential fits of the type  $C = C_0(1 - e^{-t/\tau})$ , where  $C_0$  and  $\tau$  are the saturated Au concentration and saturation time constant, respectively. Based on the experimental data and fits, a standard drive-in time of 20 h at  $750^\circ\text{C}$  was considered sufficient to saturate all the samples.

Figure 2(a) compares RBS results after 20 h Au drive-in for the HEI and HEI+I ( $+I = 9 \times 10^{13}$  and  $20 \times 10^{13}\ \text{cm}^{-2}$ ) samples. The most important features in Fig. 2(a) are: (a) the reduction of the amount of trapped Au in the region between 0.5 and 1.3  $\mu\text{m}$ , indicating that interstitials do react with the vacancies; (b) the Au concentration in the shoulder is almost constant as a function of the +I dose; and (c) the back edge of the profiles at  $\sim 1.3\text{--}1.6\ \mu\text{m}$  match up for all the doses. Features (b) and (c) indicate that there is no interstitial–vacancy reaction taking place either shallower than 0.5  $\mu\text{m}$  or deeper than 1.3  $\mu\text{m}$ , demonstrating that the +I interstitials do not escape from the 0.5–1.3  $\mu\text{m}$  region of the excess vacancy profile. These features are seen quantitatively in Fig. 2(b), which plots the dependence of the integrated Au concentrations on +I for the shoulder,  $\frac{1}{2}R_p$ , and back edge after 20 h of Au drive-in. The relatively small change in the shoulder and back edge over the whole +I dose range studied indicates that the interstitial+vacancy interaction is confined to the  $\frac{1}{2}R_p$  region.

To obtain  $k$ , the slope of the change in Au concentration

at  $\frac{1}{2}R_p$  with respect to the injected +I interstitial dose was obtained from Fig. 2(b). The slope for the  $\frac{1}{2}R_p$  Au is  $0.85 \pm 15\%$  for the 20 h Au drive-in samples, while the slope obtained by using the saturated Au concentrations from the fits of the time dependence [Fig. 1(b)] is 0.80. The close agreement between the two numbers confirms that 20 h does give the saturated value. More importantly, the slope indicates that approximately  $1.2 \pm 0.2$  interstitials are required to decrease the Au concentration by 1 atom. Under the assumptions that 1 interstitial consumes 1 vacancy and that Au reacts with all the vacancy-type defects,<sup>13</sup> this indicates that  $k$  is approximately  $1.2 \pm 0.2$  vacancies for every trapped Au atom.

The validity of the obtained factor was supported by additional experiments, as follows. (a) Cross-section TEM comparison of +I implants in the HEI sample and in bare wafers typically showed that, while no defects appeared in the HEI sample, {311}-type defects were observed for the +I dose, indicating that vacancies from the HEI suppress extended interstitial-type defect formation; (b) the  $\frac{1}{2}R_p$  of the 600 keV implants in bare Si wafers did not getter Au; and (c) loop detectors<sup>14</sup> placed at the surface confirmed that no fraction of the +I implant was lost to the surface.

From Fig. 1(a), the concentration of Au at  $\frac{1}{2}R_p$  ( $\sim 3 \times 10^{18} \text{ cm}^{-3}$ ) is seen to greatly exceed the solubility of Au at 750 °C ( $\sim 2 \times 10^{14} \text{ cm}^{-3}$ ).<sup>15</sup> Cross-section TEM was carried out on the HEI sample after 20 h of drive-in to determine the state of Au. The sample showed a distribution of precipitates of 3–15 nm in size consisting of fcc Au (determined by selected area diffraction). Additionally, no extended interstitial defects, usually observed in the case of Au–silicide precipitation<sup>16</sup> were observed. While these results suggest that metallic Au precipitates form as a result of interaction with the vacancies, the exact mechanism is still unclear. Additional features of the Au profile in Fig. 1(a), are the dips in Au concentration between 0.3 and 0.5  $\mu\text{m}$ , and the appearance of Au in the shoulder. In a simplistic approach, the dip may be explained by loss of vacancies to the surface during the anneal step after the HEI. Preliminary results on the appearance of the shoulder suggest that it may be related to knock-on implantation of surface impurities during the HEI.<sup>12</sup>

The fact that  $k$  is so close to 1 indicates that Au capture is more likely a space filling of the MeV-implant related vacancy clusters. This is in contrast to the observations of Follstaedt *et al.*,<sup>17</sup> who found that the Au concentration saturates when 1 ML of Au coats the walls of He-induced voids in Si. However, significant differences between the present experiments and those of Follstaedt, chiefly the sizes of the voids and the drive-in conditions, may account for the different observations. Currently, work is underway to deter-

mine the capture mechanism for Au by MeV-implant related vacancy clusters, especially to distinguish between mechanisms of kick-in and direct capture of Au at vacancy clusters. Nevertheless, independent of the mechanism, the Au-labeling technique provides a simple and effective tool to detect and count excess vacancies. The detection of vacancies by this technique will be limited only by the ability to detect Au in Si, while the lowest measurable vacancy concentration will be set by the solubility of Au in Si at the drive-in temperature. Subject to this, there appears no apparent impediment to extending this technique to measure vacancies produced in Si by other means.

One of the authors (R.K.) would like to thank G. Gilmer, J. Benton, and F. Baumann for stimulating discussions and help with TEM. This research was supported in part by the U.S. Department of Energy, Office of Science, Laboratory Technology Division under Contract No. DE-AC05-96OR22464 with Lockheed Martin Energy Research Corp. and Contract No. DE-AC05-76OR00033 with Oak Ridge Associated Universities.

<sup>1</sup>K. Tsukamoto, S. Komori, T. Kuroi, and Y. Akasaka, Nucl. Instrum. Methods Phys. Res. B **59/60**, 572 (1991).

<sup>2</sup>L. Rubin and W. Morris, Semicond. Int. **20**, 77 (1997).

<sup>3</sup>A. M. Mazzone, Phys. Status Solidi A **95**, 149 (1986).

<sup>4</sup>J. Y. Cheng, D. J. Eaglesham, D. C. Jacobson, P. A. Stolck, J. L. Benton, and J. M. Poate, J. Appl. Phys. **80**, 2105 (1996).

<sup>5</sup>V. C. Venezia, D. J. Eaglesham, T. E. Haynes, A. Agarwal, D. C. Jacobson, H.-J. Gossmann, and F. H. Baumann, Appl. Phys. Lett. **73**, 2980 (1998).

<sup>6</sup>O. W. Holland, L. Xie, B. Nielsen, and D. S. Zhou, J. Electron. Mater. **25**, 99 (1996).

<sup>7</sup>S. L. Ellingboe and M. C. Ridgway, Nucl. Instrum. Methods Phys. Res. B **127/128**, 90 (1997).

<sup>8</sup>C. Szeles, B. Nielsen, P. Asoka-Kumar, K. G. Lynn, M. Anderle, T. P. Ma, and G. W. Rubloff, J. Appl. Phys. **76**, 3403 (1994).

<sup>9</sup>M. Yoon, B. C. Larson, J. Z. Tischler, T. E. Haynes, J.-S. Chung, G. E. Ice, and P. Zschack, Appl. Phys. Lett. **75**, 2791 (1999).

<sup>10</sup>U. Gösele, W. Frank, and A. Seeger, Appl. Phys. **23**, 361 (1980).

<sup>11</sup>J. F. Ziegler, J. P. Biersack, and U. Littmark, *The Stopping and Ranges of Ions in Solids* (Pergamon, New York, 1985).

<sup>12</sup>We have evidence that the shoulder is also due to vacancies. For example, the Au concentration in the shoulder decreases when the energy of the +I implant is reduced to 350 keV so that some of the interstitials can escape annihilation at the  $\frac{1}{2}R_p$ . This shoulder was not seen in samples without a HEI. Quantitative findings regarding this shoulder peak will be reported in a more detailed paper to be submitted later.

<sup>13</sup>Preliminary results from positron annihilation experiments (PAS) show that the vacancy-type signal ( $S$  parameter) for a HEI sample with increasing Au drive-in time decreases as Au concentration at  $\frac{1}{2}R_p$  increases.

<sup>14</sup>J. K. Listebarger, K. S. Jones, and J. A. Slinkman, J. Appl. Phys. **73**, 4815 (1993).

<sup>15</sup>K. Graff, *Metal Impurities in Si-device Fabrication* (Springer, New York, 1995).

<sup>16</sup>F. H. Baumann and W. Schroter, Phys. Rev. B **43**, 6510 (1991).

<sup>17</sup>D. M. Follstaedt, S. M. Myers, G. A. Petersen, and J. W. Medernach, J. Electron. Mater. **25**, 151 (1996).